# Recrystallisation of Practical Mechanically Alloyed Iron–Base and and Nickel–Base Superalloys

Materials Science and Engineering A223 (1997) 64-77

H. K. D. H. Bhadeshia
University of Cambridge/JRDC
Department of Materials Science and Metallurgy
Pembroke Street, Cambridge CB2 3QZ, U.K.

**Abstract**

Commercialised mechanically alloyed yttria dispersion strengthened alloys exhibit unusual recrystallisation behaviour. In spite of their large stored energy content, they tend to recrystallise at temperatures close to melting. The recrystallised microstructure is often very coarse and highly anisotropic, characterised by columnar grains. Such a microstructure is often referred to as being "directional recrystallised". This and other features of these unique alloys are reviewed. It is found that many of the observed peculiarities can be attributed to the ultra–fine grained structure present prior to the recrystallisation heat–treatment. In some cases the manufacturing process tends to align the dispersoid particles along the principal fabrication direction. This in turn encourages recrystallisation to be directional.

## INTRODUCTION

Some of the most successful mechanically alloyed materials include the oxide dispersion strengthened iron–base and nickel–base superalloys. Their recrystallisation behaviour is peculiar and is the subject of this review. During heat treatment of the consolidated mechanically alloyed (MA) powders, the bulk samples recrystallise into remarkably anisotropic and coarse columnar grain structures. In addition, recrystallisation usually does not occur until temperatures close to melting are reached [1–3].

The mechanical alloying process itself has been reviewed elsewhere [1–4]. Briefly, it involves the creation of an alloy by the intense mechanical deformation of mixtures of elemental or master–alloy powders (Fig. 1). The powders are then consolidated by various combinations of hot–isostatic pressing and extrusion; the alloys in this condition are usually too hard to use. They are therefore heat–treated, either isothermally or in a temperature gradient to induce recrystallisation. Mechanical alloying permits the usual limits of solubility imposed by solidification to be exceeded, but in addition, dispersoid particles (such as oxides) can be introduced uniformly into bulk materials. It is this latter facility which has led to commercial exploitation on a large scale. The mechanical alloying process is a relatively difficult manufacturing method. Variations in processing conditions (which are seldom revealed) can completely change the subsequent properties of the alloys. For this reason, we concentrate here on alloys which are considered to be established commercially and which therefore should have reproducible properties.

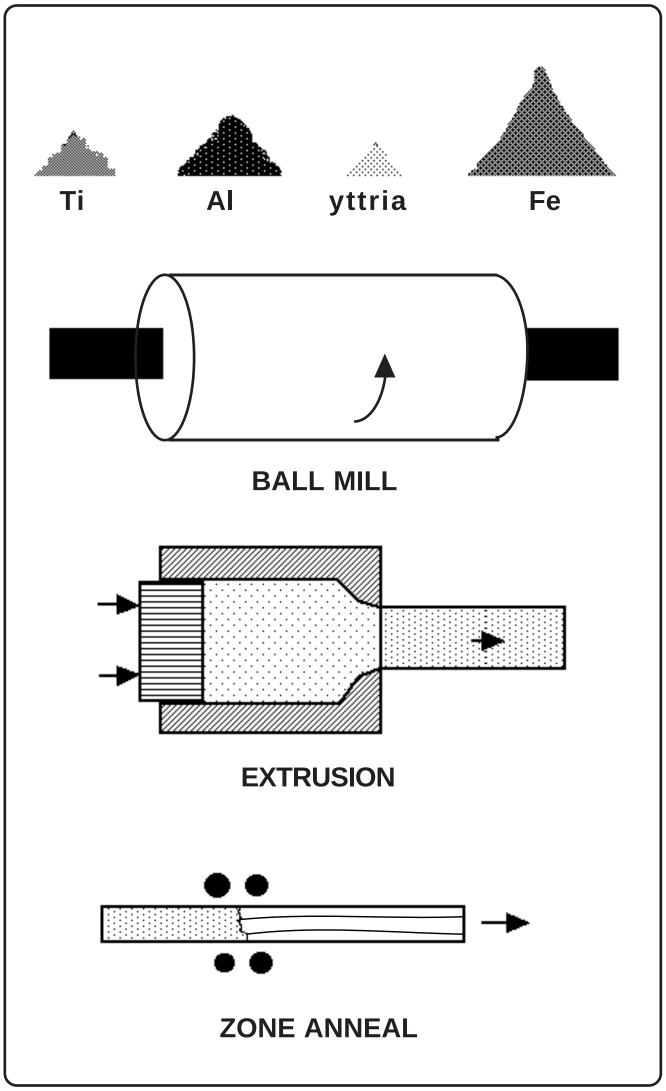


Fig. 1: A schematic illustration of a common method of manufacturing large quantities of mechanically alloyed metals for engineering applications. The elemental powders/master–alloys/oxides are milled together to produce solid solutions with oxide dispersoids. This powder is then consolidated and the resulting bulk alloy heat–treated to achieve a coarse, directional grain structure.

This review begins with an introduction to the range of important commercial alloys, followed by an assessment of their strange recrystallisation behaviour. There are two main classes of mechanical alloys which are of commercial significance, the oxide dispersion strengthened

| Steels | C | Cr | Al | Mo | Ti | N | | $Ti_2O_3$ | $Y_2O_3$ | Fe |
|---|---|---|---|---|---|---|---|---|---|---|
| MA957 | 0.01 | 14.0 | – | 0.3 | 1.0 | 0.012 | | – | 0.27 | Balance |
| DT2203Y05 | | 13.0 | – | 1.5 | 2.2 | | | – | 0.5 | Balance |
| ODM 331 | | 13.0 | 3.0 | 1.5 | 0.6 | | | – | 0.5 | Balance |
| ODM 751 | | 16.5 | 4.5 | 1.5 | 0.6 | | | – | 0.5 | Balance |
| ODM 061 | | 20.0 | 6.0 | 1.5 | 0.6 | | | – | 0.5 | Balance |
| MA956 | 0.01 | 20.0 | 4.5 | – | 0.5 | 0.045 | | – | 0.50 | Balance |
| PM2000 | $< 0.04$ | 20.0 | 5.5 | | 0.5 | | | – | 0.5 | Balance |
| PM2010 | $< 0.04$ | 20.0 | 5.5 | | 0.5 | | | – | 1.0 | Balance |
| DT | | 13.0 | – | 1.5 | 2.9 | | | 1.8 | – | Balance |
| DY | | 13.0 | – | 1.5 | 2.2 | | | 0.9 | 0.5 | Balance |

| Ni–Base | C | Cr | Al | Ti | W | Fe | N | Total O | $Y_2O_3$ | Ni |
|---|---|---|---|---|---|---|---|---|---|---|
| MA6000 | 0.06 | 15.0 | 4.5 | 2.3 | 3.9 | 1.5 | 0.2 | 0.57 | 1.1 | Balance |
| MA760 | 0.06 | 19.5 | 6.0 | – | 3.4 | 1.2 | 0.3 | 0.6 | 1.0 | Balance |
| MA758 † | 0.05 | 30.0 | 0.3 | – | 0.5 | – | – | 0.37 | 0.6 | Balance |

Table 0: Compositions (wt.% ) of some typical alloys. † MA758 is a nickel base mechanical alloy without $\gamma'$ strengthening. The compositions of ODM061, DT and DY are from Regle [5], as are the nitrogen data for MA956 and MA957. The compositions of PM2000 and PM2010 are from Krautwasser *et al.* [6].

(ODS) iron–base superalloys and the ODS nickel–base superalloys †.

*Iron–Base Alloys*

These alloys (Table 1) are designed to be oxidation and corrosion resistant, but with a greater creep strength when compared with equivalent cast alloys, due to the dispersion of fine yttria particles. MA956 has the greater oxidation resistance due to the higher chromium

† The following trade names are used throughout the text: MA956, MA957, MA6000 and MA760 are alloys manufactured by INCO; the ODM series, DT and DY are alloys manufactured by Dour Metal (the term *ODM* originates from the phrase *oxide dispersion strengthened microforged*). The alloy DT2203Y05 has been developed by CEN/SCK of Belgium; PM2000 and PM2010 are alloys developed by Plansee of Austria (they were during the development stage also known by the designations F10 and F11 respectively).

concentration, and its large aluminium content. The presence of yttria suppresses the spalling of the protective alumina films by trapping sulphur at the particle/matrix interfaces and hence reducing its segregation to the oxide/metal interface [Ikeda *et al.*, 1995]. All of the steels listed are supposed to be ferritic. Normal ferritic steels tend to undergo a marked loss in creep strength at temperatures in excess of 600 °C; the ODS alloys discussed here can in principle be used at much higher temperatures.

The ferritic state also makes the iron–base alloys less susceptible to radiation induced swelling. MA957 and a similar steel DT2203Y05 are therefore designed for nuclear reactor applications, for use in a liquid sodium environment at temperatures of the order of 700 °C. Both have a high void swelling resistance, and a low carbon concentration in order to avoid the formation of titanium carbides. The titanium is meant to combine with chromium, molybdenum and iron to form a stable b.c.c. FeCrTiMo intermetallic $\chi$–phase during ageing at around 800 °C, which can further boost the creep strength. The rupture strength of ODM751 is larger than that of MA956 [7]. ODM751 has an additional 1.5 wt.% Mo which, either via the $\chi$–phase or through solid solution strengthening, presumably adds to the creep strength of ODM751. However, the results are confusing because PM2000, which does not contain molybdenum, virtually matches the rupture strength of ODM751.

*Nickel–Base Alloys*

The nickel–base alloys MA6000 and MA760 are both $\gamma'$ strengthened, as in conventional nickel–base superalloys; the dispersion strengthening with yttria allows the strength to be maintained to much higher temperatures. For example, at 1093 °C, the 1000 hour rupture strength of MA6000 is twice that of conventional nickel–base superalloys. For reasons which are not clear, the (low and high cycle) fatigue resistance of MA6000 is much better than that of conventional alloys, as is its thermal fatigue resistance [2].

A lot of the oxidation resistance of MA6000 relies on the formation of chromia at the surface. However, chromia is not very resistant to sulphidation. Resistance to sulphide attack is important in industrial gas turbine manufacture, where the ODS alloys have applications as vanes. MA760 has a higher sulphidation and oxidation resistance, due to its higher chromium and aluminium concentrations, the latter inducing the formation of surface alumina [8].

The reported solidus temperatures and densities of some of the alloys are listed in Table 2. Similar data do not seem to be available in the published literature for the other alloys listed in Table 1. There is nothing unusual in these data, but they are relevant in two respects. Firstly, it will be seen later that the recrystallisation temperatures of both the iron and nickel base alloys are generally close to the temperature at which melting begins. Secondly, the mechanical alloying and subsequent consolidation process leads to a density which cannot, within the limits of experimental error, be distinguished from that obtained by conventional casting and solidification.

| Alloy | Solidus Temperature / °C | Density $\text{g cm}^{-3}$ | References |
|---|---|---|---|
| MA956 (Fe base) | 1482 | 7.2 | INCO datasheet |
| MA956 (Fe base) | | 7.12 | Regle [5] |
| MA957 (Fe base) | $\simeq$ 1500 | 7.62 | Regle [5] |
| MA758 (Ni base) | 1350 | 8.14 | Sha & Bhadeshia [9] |
| | | | INCO datasheet |
| MA760 (Ni base) | 1295 | 7.89 | Sha & Bhadeshia [9] |
| | | | INCO datasheet |
| MA6000 (Ni base) | 1296 | 8.11 | INCO datasheet |

Table 2: Some physical data for common alloys

## INITIAL MICROSTRUCTURES

Immediately after the mechanical alloying process, the powders are canned and extruded/hot–rolled to produce the appropriate bulk forms of the alloys. The as–mechanically alloyed materials have a grain size which can be as fine as 1–2 nm locally. During heating for either extrusion or rolling, the canned mechanically alloyed powders may recrystallise to a sub–micron grain size which is representative of the grain structure found immediately after consolidation (Fig. 2). These incredibly fine grain sizes are a consequence of the strains imparted on the powders during the mechanical alloying process, true strains of the order of 9 (equivalent to stretching a unit length by a factor of 8000). The subsequent consolidation by comparison involves minor degrees of deformation, but much higher bulk temperatures (around 1000 °C). It is known that during the course of consolidation, the material may dynamically recrystallise several times. It should be emphsized that the sub–micron grains referred to above are true grains with large relative misorientations, not simply dislocation cell structures generated by deformation.

Nevertheless, the iron–base alloys immediately after consolidation have a cold–deformed microstructure in which the ultra–fine grains are elongated along the working direction and contain other classic features of cold work, *i.e.* the high dislocation density and a generally convoluted microstructure. The dislocation density has been measured for DT2203Y05 to be about $10^{15}$ $\text{m}^{-2}$ [10]; although this is large, it is not particularly high when compared with dislo-

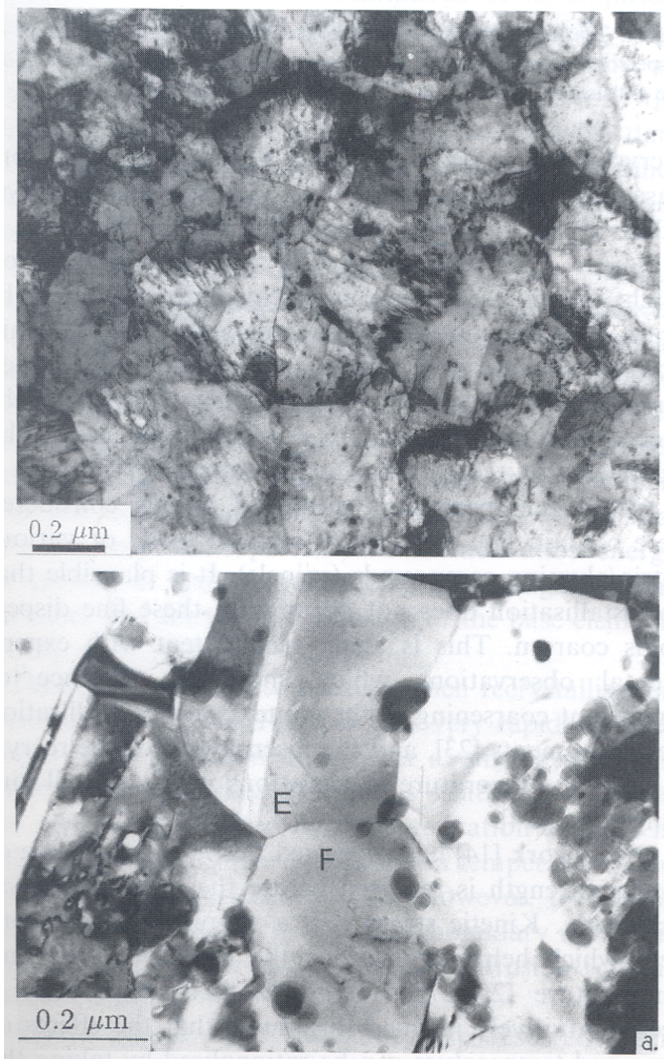


Fig. 2: Transmission electron micrographs showing the sub–micron grain structure of mechanically alloyed and consolidated alloys. (a) Iron–base MA956. (b) Nickel–base MA6000; electron diffraction confirms that there are large misorientations across grains such as $E$ and $F$. The grains in both cases do not represent low–misorientation cells of the type common in ordinary deformation. Both micrographs are sections normal to the extrusion direction. The appearance of MA6000 microstructure is independent of the plane of section, but the microstructure of MA956 is cold–deformed and hence the grains are elongated along the extrusion direction.

cation densities found in conventional steel martensitic microstructures (Fig. 3a). Subsequent heat–treatment leads to primary recrystallisation into a very coarse grained microstructure (Fig. 3b).

The nickel–base superalloys also have an ultra–fine grained microstructure, but one which is the product of primary recrystallisation (Fig. 2b). The sub–micrometer grains are therefore equiaxed, contain undistorted annealing twins and a clean microstructure. Subsequent heat treatment therefore leads to secondary recrystallisation driven by the grain boundary energy of the fine grained primary recrystallised state. It is not clear why the nickel base alloys are in a primary recrystallised state following extrusion/hot–rolling, whereas the iron–base alloys,

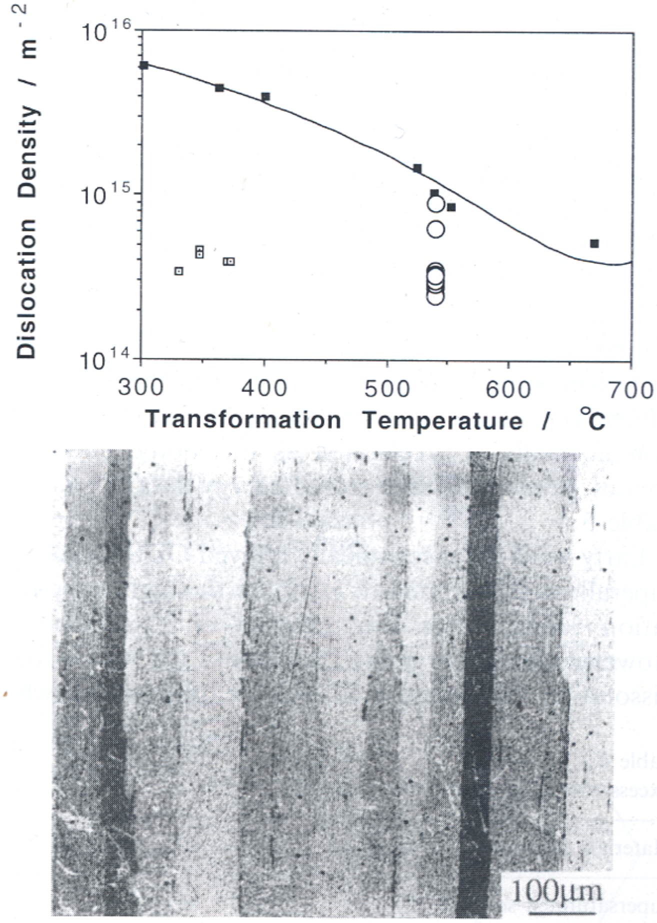


Fig. 3: (a) The measured dislocation densities as a function of the transformation temperature in low–alloy steels. The microstructures range from Widmanstätten ferrite, bainite, acicular ferrite and martensite [11,12]. (b) An optical micrograph showing a typical directionally recrystallised grain structure. The alloy concerned is MA956, but the microstructure is broadly representative of all of the alloys listed in Table 1.

which are fabricated under identical conditions, have a cold deformed microstructure.

Irrespective of whether the alloys have a primary or secondary recrystallised microstructure, the ultra–fine grains obtained after recrystallisation make the alloys very hard (Table 3) and for most applications unusable without heat treatment which leads to an enormous coarsening of the microstructure with a reduction in the amount of grain surface per unit volume by 2–3 orders of magnitude. The details of recrystallisation are discussed in the next section.

The excess energy stored in the mechanically alloyed and consolidated materials described in Table 1 is primarily in the form of grain surfaces and to a lesser extent due to dislocations and other high–entropy defects. We shall see later that this stored energy amounts to about

| Alloy | HV, Before Recrystallisation | HV, After Recrystallisation |
|---|---|---|
| MA957 | 400–410 | 230–240 |
| MA956 | 350–390 | 225–245 |
| MA956 Sheet | 410 | 250 |
| MA6000 | 645 | 500–520 |
| MA760 | 720–790 | 500–515 |
| MA758 | 405 | 214 |

Table 3: Typical Vicker's Hardness data before and after recrystallisation into a coarse grained microstructure.

1 J $g^{-1}$ in spite of the sub–micron grain size. Although this value is much larger than that in normal cold–deformed materials, it is much smaller than in many metastable materials. This is because the commercial alloys do not contain more solute than can be tolerated by the matrix – the mechanical alloying process is not used commercially to trap excess solute, but primarily to introduce stable oxide dispersions. Table 4 lists the excess energies of some metastable materials in units of $RT_M$, where $R$ is the gas constant and $T_M$ the absolute melting temperature. Thus, a unit value corresponds approximately to the thermal energy available at the melting temperature. It is evident that the commercial alloys are not particularly metastable in this context.

| Materials Example | $\mathrm{RT_M}$ units |
|---|---|
| Supersaturated Solution | $< 1$ |
| Intermetallic Compounds | $< 0.5$ |
| Amorphous Solids | $< 0.5$ |
| Compositionally Modulated Films | $< 0.1$ |
| Interphase Dispersions | $< 0.1$ |
| Commercial Mechanical Alloys | $< 0.005$ |

Table 4: Excess energy in metastable materials. Some of the data are from Turnbull [13]. The supersaturated solution is one in which solute has been trapped against equilibrium.

Extrusion/rolling leads to an alignment of dispersoid particles along the working direction, the degree of alignment being pronounced in the case of the iron–base alloys [14] Fig. 4. This alignment reflects inhomogeneities in the fabrication process arising at the single particle level and below. Thus, the iron–base alloys almost always tend to recrystallise into a columnar grained microstructure, with the principal growth direction being parallel to the extrusion direction, irrespective of whether the sample is zone annealed, cross annealed or isothermally treated. (Cross annealing is zone annealing along a direction normal to the extrusion direction). For reasons which are not clear, the anisotropy in particle dispersion is much less for the nickel base superalloys, in which the direction of columnar grain growth can often be controlled by the sense of the temperature gradient during zone annealing. Indeed, equiaxed coarse grained secondary recrystallised microstructures can be readily generated either by isothermal annealing or by zone annealing at high speeds [15].

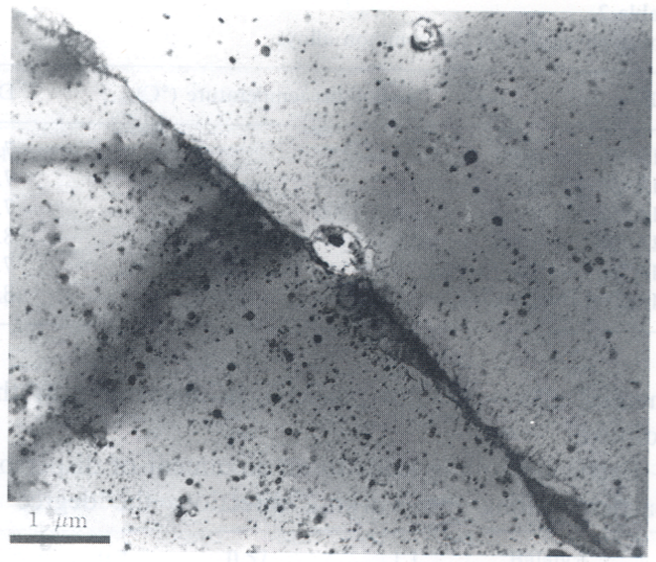


Fig. 4: Transmission electron micrograph showing the alignment of dispersoid particles in MA956. The rows of particles are parallel to the extrusion direction identified by the grain boundary

## THE RECRYSTALLISATION TEMPERATURE

The recrystallisation of mechanically alloyed yttria dispersion strengthened steels and nickel–base superalloys occurs at exceptionally high homologous temperatures, of the order of 0.9 of the melting temperature ($T_M$). This contrasts with recrystallisation at about 0.6 $T_M$ in ordinary variants of similar metallic alloys. Strangely enough, the mechanically alloyed metals contain a more stored energy than in conventional materials which recrystallise at lower temperatures; recrystallisation normally is accelerated as the stored energy increases. Some measured stored energy data are listed in Table 5.

| Alloy | Stored Energy J $g^{-1}$ | Heating Rate K $min^{-1}$ | Comment |
|---|---|---|---|
| MA957 | 1.0 | | Primary Recrystallisation |
| MA956 | 0.4 | | Primary Recrystallisation |
| MA956 sheet | $\simeq 0.4^{\dagger}$ | | |
| MA6000 | 0.6 | | Secondary Recrystallisation |
| MA760 | 1.0 | 30 | Secondary Recrystallisation |
| MA758 | 0.3 | 10 | Secondary Recrystallisation |

Table 5: Enthalpy of Recrystallisation [9,16,17,18]. $^{\dagger}$: in MA956 sheet, the stored energy is released over a relatively large range of temperatures and is difficult to measure accurately. For MA758 the stored energy is small and recrystallisation occurs close to the melting point making the stored energy difficult to measure.

Early work on mechanically alloyed ODS nickel–base superalloys [19] tended to attribute the high recrystallisation temperatures the presence of $\gamma'$ precipitates. However, there are many such alloys for which the $\gamma'$ dissolution temperature is well below that at which recrystallisation occurs [20,21,22]. Furthermore, the iron–base alloys do not contain any $\gamma'$ and yet also recrystallise at similarly high temperatures.

It has been speculated [23] that recrystallisation might be initiated when at elevated temperatures the grain boundary mobility suddenly rises because grain boundary solute drag effects are overcome at elevated temperatures. This is inconsistent with the fact that the recrystallisation temperature can be altered greatly by relatively low–temperature heat treatments [16].

All of the mechanically alloyed metals considered here contain fine particles of yttrium oxide or various yttria/alumina compounds (spinels). It is plausible that recrystallisation does not occur until these fine dispersoids coarsen. This is again inconsistent with experimental observations which show the absence of significant coarsening in the context of recrystallisation heat treatments [24], and the insensitivity of the recrystallisation temperature to variations in the overall pinning force [25].

Other work [15] has suggested that a critical value of kinetic strength is required before the onset of recrystallisation. Kinetic strength is a simple empirical concept which helps to combine the effects of time and temperature [26,27,28]. For an isothermal process, it seems intuitively justified to assume that the effects of time and temperature can be rationalised by taking the product:

$$t \exp\{-Q/kT\} \tag{1}$$

where $t$ is the heat treatment time, $Q$ is an activation energy and the other terms have their usual meanings. This concept can be generalised to anisothermal heat treatments by taking the integral:

$$\int \exp\{-Q/kT\{t\}\}\ dt \tag{2}$$

over the cycle of interest. Although the method has been successful within the limitations of its empirical character, it fails to explain the unexpectedly high recrystallisation temperatures in the mechanically alloyed metals. The activation energy $Q$ needed in the kinetic strength function, to rationalise available data on any particular alloy turns out to be some ten times greater than that for the self diffusion of the base element.

More fundamental methods of analysing overall transformation kinetics are based on the Johnson–Mehl–Avrami method, which can be developed to as much rigour as is necessary, or as the need to know certain parameters permits. One simplification often used is to ignore nucleation by assuming that a fixed number of nucleation sites exists at time zero. If this is done for the mechanical alloys, then the experimental data are only well represented if the activation energy for growth is made unrealistically large (again, some ten times that for the self diffusion of the base element) [25,29].

These difficulties arise because when recrystallisation occurs at around 0.9 $T_M$, it occurs very rapidly during isothermal heat treatment, or over a very narrow temperature range during continuous heating. Such data can only be represented by large activation energies in order to achieve high recrystallisation temperatures and rapid subsequent transformation. However, to assume that the activation energy for grain boundary motion is very much greater than that for self–diffusion ($Q_D$) is unconvincing.

Almost all of these difficulties are resolved when nucleation is considered in detail [29,30]. It turns out that the activation energy for *nucleation* in the mechanical alloys should indeed be very large. This is because the alloys have an unusually small grain size prior to recrystallisation. The nucleation of recrystallisation occurs by the bowing of grain boundaries, a process which for conventional alloys is straightforward since the distance between grain boundary junctions is usually larger that between other strong pinning points. With the sub–micrometer grain size of mechanically alloyed metals, the grain junctions themselves act as severe pinning lines for grain boundary bowing (Fig. 5). It is easy to demonstrate that this should lead to an enormous activation energy for the nucleation of recrystallisation, many orders of magnitude larger than $Q_D$. It should be noted that $Q$ in this model might be reduced if a few grains happen to be slightly larger than others (either because adjacent grains are similarly orientated or because of local variations due to the uncertainties in the mechanical alloying process).

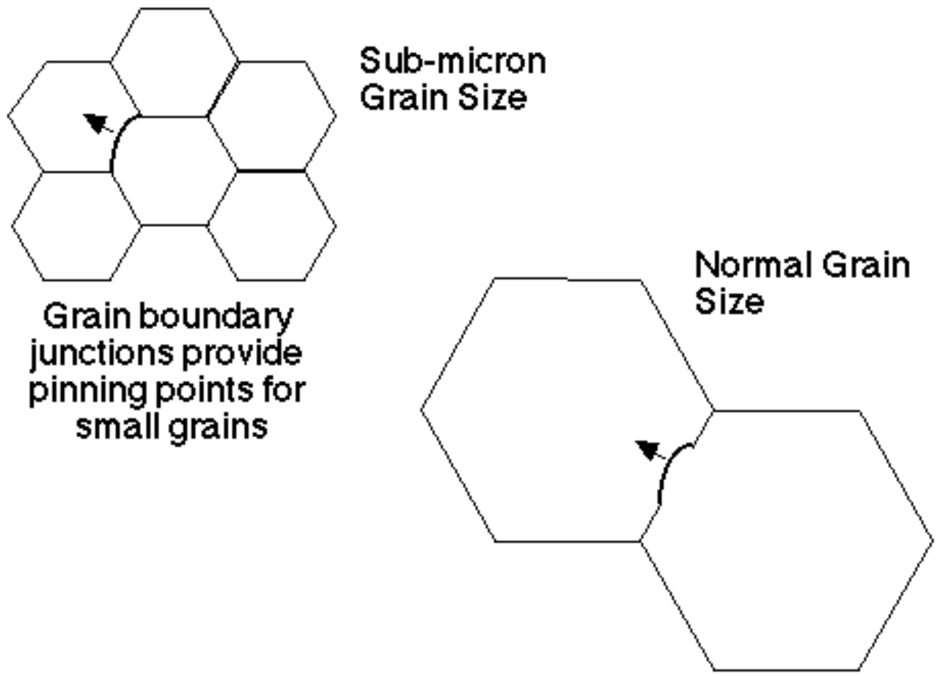


Fig. 5: The nucleation of recrystallisation occurs by the formation of a grain boundary bulge. This can occur with less constraint when the grain junctions are spaced at distances greater than the critical bulge size. With the ultra–fine grains of mechanically alloyed metals, the grain junctions are themselves pinning points, making it very difficult to form large enough bulges.

This model for nucleation suggests a new concept, that individual grains cannot be considered to be topologically independent when the grain size becomes sufficiently small. It has some remarkable consequences which have been verified experimentally:

(a) The model explains the high homologous recrystallisation temperatures irrespective of alloy system. Recrystallisation is retarded whenever the grain size is small enough for the grain junctions to act as pinning points during the formation of viable nuclei in the form of grain boundary bulges.

(b) The model predicts that the recrystallisation temperature should decrease if the the stored energy is reduced by a low–temperature heat treatment which leads to uniform grain coarsening. This has now been verified experimentally for several alloys [16,29]. Since recrystallisation should eventually become more difficult as the stored energy is reduced, the curve of recrystallisation temperature versus grain size (or stored energy) should show a minimum. This prediction has been verified experimentally [29].

## ROLE OF CRYSTALLOGRAPHIC TEXTURE

Studies of the effect of the crystallographic texture in consolidated MA ODS alloys on their recrystallisation behaviour have been confined to the iron–base alloys. There is conclusive evidence that the recrystallisation temperature can be sensitive to the initial texture. A reasonable explanation for this is that grain boundary mobility is affected by texture. During the directional recrystallisation of ultra–fine grained MA ODS alloys, the recrystallised grains are usually several hundreds of microns in width, and advance into a matrix with sub–micrometer sized grains. Thus, the recrystallisation front in effect "sees" a tremendous variety of crystallographic orientations and might be regarded as advancing into a liquid like structure. It then is reasonable that samples in which the grains are oriented high mobility along the extrusion direction, recrystallise more readily.

Crystallographic texture data suggest that when there is a preferred distribution of orientations, the major components of texture in the mechanically alloyed steels are $\{001\} < 110 >$, $\{111\} < \overline{1}10 >$ [31,32], which belong to the so–called $\alpha$ and $\gamma$ fibres in crystal orientation distribution space. This applies in both the states, before and after recrystallisation, the recrystallisation process simply changing the strength of the texture components with respect to a random distribution of orientations. For reasons which are not obvious, recrystallisation seems easiest whenever the $\{111\} < \overline{1}10 >$ is prominent (Table 6). Thus, MA956 prior to recrystallisation is rich in this particular component whereas MA957 is not, probably due to the presence of austenite in MA957 at the fabrication temperature [16]. The former has a substantially lower recrystallisation temperature compared with the latter, even though MA957 has a relatively higher stored energy and lower yttria content than MA956. However, if MA957 is pre–annealed (*i.e.* heat–treated without recrystallisation) in order to make its texture comparable to that of MA956, then its recrystallisation temperature drops in spite of the reduction in stored energy due to the preannealing heat–treatment.

Evens *et al.* [33] have also conducted microtextural measurements, and interpreted their recrystallisation results in terms of the different mobilities of grain boundaries with different orientations.

To summarise, there is no doubt that texture can influence the recrystallisation charac-

| | As–Received MA956 | As–Received MA957 | Preannealed MA957 |
|---|---|---|---|
| Stored Energy $\mathrm{J\,g^{-1}}$ | 0.4 | 1.00 | 0.70 |
| Recrystallisation Start<br>Recrystallisation Finish | 1273 °C<br>1334 °C | 1429 °C<br>1447 °C | 1362 °C<br>1382 °C |
| Texture Summary | $\{111\} < \bar{1}10 >$<br>$\{001\} < 110 >$ | Random<br>Random | $\{111\} < \bar{1}10 >$<br>$\{001\} < 110 >$ |
| Recrystallised Grains | Highly anisotropic | anisotropic | Equiaxed fine |

Table 6: Recrystallisation characteristics of MA956 and MA957 in the as–received condition [17]

teristics, but the mechanism remains unclear. There are many data in the literature which show that the stored energy varies with the texture components, but those data are not relevant in the present context because contrary to the results of conventional recrystallisation experiments, the reduction in recrystallisation temperature is accompanied by a reduction in stored energy. It could be argued that the particular component $\{111\} < \bar{1}10 >$ gives a higher grain boundary mobility within a liquid–like matrix of ultra–fine grains, but this explanation remains speculative.

## THE DISPERSOIDS AND PRECIPITATES

Fine yttria particles ($\simeq 10$ nm) are incorporated into the metallic matrix as a consequence of the ball milling operations. Most of these survive as yttrium oxide in spite of consolidation by extrusion and rolling at about 1050 °C. However, heat–treatment causes these particles to react with dissolved aluminium (or titanium) and oxygen to produce a variety of compounds [6,25,34,35]. The possible combinations of yttria and alumina include those listed in Table 7.

| | | |
|---|---|---|
| $3Y_2O_3.5Al_2O_3$ | YAG | yttrium aluminium garnet |
| $Y_2O_3.Al_2O_3$ | YAH | yttrium aluminium hexagonal |
| $2Y_2O_3.Al_2O_3$ | YAM | yttrium aluminium monoclinic |
| $Y_2O_3.Al_2O_3$ | YAP | yttrium aluminium perovskite |
| $Y_2O_3.Al_2O_3$ | YAP' | yttrium aluminium pseudo–perovskite |
| $3Y_2O_3.5Al_2O_3$ | YAT | yttrium aluminite tetragonal |

Table 7: Yttrium–Aluminium–Oxygen compound reported to occur in mechanically alloyed ODS iron and nickel base alloys.

The alumina particles tend to be some 500 nm in size, the titanium carbonitrides about 100–200 nm in size [5], and both have a much smaller number density than the original yttria particles. Hence, the reaction does not lead to a significant coarsening of the size distribution or inter–particle spacing. Even extremely severe heat–treatment (72 hours at 1400 °C) has little effect on the yttrium containing particles [24]. Typical changes in the size of the finer particles are illustrated in Fig. 6, which represents data for samples annealed for 110 h at the temperatures indicated, for samples of PM2010 [6]. Note that these data do not represent coarsening driven by interface energy minimisation, but complicated effects originating in the reactions between the yttria, aluminium and oxygen. Thus, the volume fraction is not constant during heat treatment. The volume fraction of the smaller reactive particles increases, whereas any large alumina particles tend to dissolve as the aluminium reacts with the yttria [6].

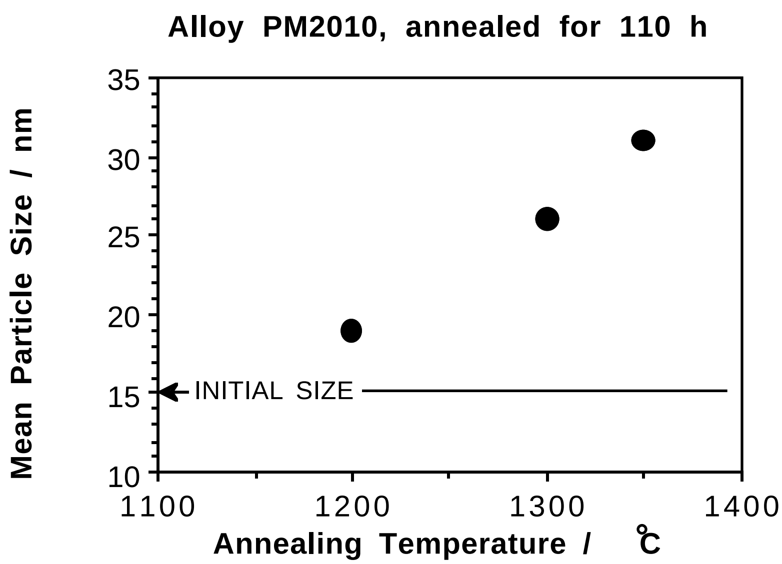


Fig. 6: Changes in particle size due to annealing, of alloy PM2010, for 110 h at each of the temperatures indicated. Data from Krautwasser *et al.* [6]

In the extruded condition, 80 % of the particles in both MA956 and MA957 are less than 15 nm in size, with those in MA956 being much smaller [5]. Nevertheless, the mean particle diameters are quite similar at 11.7 and 11.4 nm for MA957 and MA956 respectively [5], presumably because the fraction of particles is larger in the latter. Some typical particle sizes for the fine particles are presented in Table 8.

Almost all the mechanical alloys contain alumina particles introduced accidentally or as a consequence of internal oxidation during mechanical alloying (alumina is deliberately added to

| Alloy | Mean Particle Size / nm | Reference |
|---|---|---|
| MA957 | 12 | Regle [5] |
| MA956 | 12 | Regle [5] |
| MA956 | 20 | Hupalo *et al.* [**] |
| PM2010 | 15 | Krautwasser *et al.* [6] |

Table 8: Some particle characteristics, with the alloys in the unrecrsytallised "as–received" condition.

ODM751 at the mechanical alloying stage). These particles are also stable, but are too coarse and few to cause significant Zener pinning. Titanium containing mechanical alloys such as MA957 and MA6000 also contain titanium–rich particles whose exact character is not known; they may be oxides or carbo–nitrides.

The coarsest precipitates, which are not very stable, are the $M_{23}C_6$ particles which are visible optically, and dissolve (at around 1000 °C) during heating to the recrystallisation temperature only to reprecipitate during slow cooling to ambient temperature. These carbides are found in the nickel–base superalloys and not in the iron–base alloys which contain very low carbon concentrations.

To summarise, the yttrium based dispersoids are extremely stable in spite of some reaction with aluminium and oxygen to form garnets. The other particles are likely to be of little consequence to both the recrystallisation process and the creep resistance of the alloys.

The mechanism by which the fine yttrium containing particles enhance the creep resistance has been studied both for the mechanically alloyed nickel–base superalloys and the steels [36–39]. The creep resistance arises from the fact that dislocations have to climb over the hard obstacles. For steels, the consequent improvement in creep resistance allows alloys such as DT2203Y05 to be used at a service temperature of 975 K compared with that for conventional ferritic stainless steels whose maximum service temperature is about 925 K.

For the steels, there is some evidence that the oxide particles and the intermetallic compounds which precipitate in some alloys, inhibit the migration of boundaries (Evans *et al.*, 1992).

## EFFECT OF YTTRIA CONTENT

It might be assumed that an increase in the yttria content should lead to a corresponding increase in the creep resistance. This must be the case as the concentration is increased from zero, but recent work [6] indicates that there may be an optimum concentration of yttria. In a series of experiments carried out on alloys PM2000 and PM2010, which differ only in the yttria content (0.5, 1.0 wt.% respectively), it was found that the higher yttria content of PM2010 does not lead to a significantly larger number density of fine dispersoids ($<$ 100 nm). It was predicted therefore that PM2010 should not have a higher creep strength than PM2000 [6]. This result remains to be verified.

It also appears that in iron base alloys, yttria contents in excess of 0.5 wt.% cause a deterioration in oxidation resistance because of a change in the morphology of the oxide [41].

## THE GRAIN SHAPE

The major peculiar feature of the ODS mechanical alloys is that they tend to recrystallise into a highly anisotropic columnar grain structure. There are two reasons why such grain structures should arise. Zone annealing, like directional solidification can encourage growth along the associated moving temperature gradient. Secondly, any dispersoids may tend to align along the extrusion direction, so that the Zener pinning force is smallest for growth parallel to the working direction, for both MA957 and MA956.

The nickel base alloys do not have a pronounced nonuniform distribution of dispersoids. Thus, MA6000, when isothermally annealed, often recrystallises into an equiaxed grain structure (there are batch–to–batch variations). The same alloy will recrystallise directionally when zone annealed. The sense of the columnar grains can be altered by changing the zone annealed direction; cross annealing (*i.e.* zone annealing in a direction normal to the extrusion direction) causes the growth of stubby columnar grains normal to the extrusion direction, confirming a more or less uniform dispersoid distribution. In addition, zone annealing at high speeds leads to a transition from a columnar to equiaxed recrystallised grains [15].

The nickel base alloy MA760 has a response which is similar to that of MA6000, although the signs are that there is a stronger alignment of particles along the extrusion direction. Thus, isothermal annealing does not lead to equiaxed grains, but cross annealing can change the direction of the columnar recrystallised grains.

The mechanically alloyed steels contain a very pronounced alignment of particles along the extrusion direction. Isothermal heat–treatment of as–worked samples always leads to the development of coarse columnar grains. MA957, which has a rather low yttria content, has relatively stubby columnar grains following isothermal heat treatment. No amount of cross annealing or any other heat treatment has succeeded in causing a change in the direction of columnar grain growth, which is always parallel to the working direction. The importance of a nonuniform dispersion of particles in inducing the development of columnar grains has been emphasized in recent experiments where the introduction of HfC or $TiB_2$ led to the formation of anisotropic grains during secondary recrystallisation of the NiAl intermetallic matrix [42].

The roughness of grain boundaries in recrystallised mechanically alloyed nickel–base superalloys and steels has been characterised in detail [43–45]. The serrated boundaries arise because of transient pinning by dispersoids. Coarser and smoother boundaries occur when the stored energy is large, simply because it is then easier for the boundary to overcome the pinning force [45].

## PREANNEALING EFFECTS

Preannealing is a term used to describe a sample which has been heat treated at a temperature which is too low for recrystallisation, but high enough to induce significant changes in the stored energy, and in the subsequent microstructure following an elevated temperature recrystallisation heat treatment.

The effects of preannealing, at temperatures above that at which austenite can form, on MA957 can be summarised as follows [16]. A weak preannealing treatment (at about 1150 °C) has little or no effect on subsequent recrystallisation. As the preannealing time is increased, there is a transition from a coarse columnar grain structure to one which is equiaxed (20–40$\mu$m) depending on the exact heat treatment). This is because the reduction in stored energy reduces grain boundary mobility, so that nucleation has an opportunity to develop in several regions of the sample, giving an equiaxed grain structure.

Continued preannealing causes the development of a bimodal equiaxed grain structure. This is because there is an inhomogeneous distribution of pinning particles in the alloy. The now substantial reduction in stored energy due to preannealing, retards recrystallisation more in some regions compared with others which are less strongly pinned. For MA957 the preannealing time at 1150 °C is in excess of 160 hours for this condition to be reached.

Further preannealing leads to such a large reduction in the stored energy that subsequent recrystallisation is suppressed.

It is much more difficult to control the grain structure of MA956 using preannealing heat treatments. Grain refinement certainly occurs, as in MA957, but the fine grains tend not to be equiaxed. This may be because MA956 contains a larger concentration of yttria. The anisotropic pinning due to the inhomogeneous distribution of the oxide particles is more difficult to overcome if the fraction of particles is large. It would be very interesting to test this with MA956 containing a smaller quantity of yttria dispersoids.

## VOID SWELLING RESISTANCE: FERRITIC ALLOYS

The formation of voids during irradiation causes the swelling of metals. A discussion of such effects is included here for interest. Irradiation tends to cause the formation of both interstitials and vacancies in equal concentrations, but the former anneal out more rapidly than the latter. The resulting excess vacancy concentration can condense out to form voids.

The subject has been reviewed by Little [46]. It seems that ferritic steels have a much higher resistance to void swelling than austenitic alloys, although nickel base alloys rank alongside the ferritic steels. Point defects introduced by irradiation can condense at *neutral* or *biased* sinks. The latter are typically dislocations with large Burgers vectors and attract more interstitials than vacancies, leaving an excess of vacancies to form voids. Hence, anything which encourages neutral sinks makes for a high void swelling resistance.

It is believed that in ferritic steels, irradiation induces two kinds of dislocations, one which is strongly biased and the other which is neutral. Hence there are effective sinks for both interstitial and vacancy point defects, thereby leading to a smaller excess of vacancies capable of forming voids.

However, there are significant variations in the void swelling resistance over the range of available creep resistant ferritic steels. For a given vacancy concentration, a larger number density of vacancy traps is conducive to a smaller tendency for swelling. Lath boundaries or the yttrium oxide particles in the mechanically alloyed steels are good vacancy traps. Hence, the latter alloys have very satisfactory void swelling resistance [46].

Some typical data comparing a mechanically alloyed ODS steel DT2203Y05 with a corresponding conventional ferritic steel AISI 410 (Fe–12Cr–0.4Ni–0.4Mn–0.2Si–0.1C wt.%) are given in Table 9 [10]. It is obvious that the mechanical alloy is able to accommodate a lot more helium and that it has a relatively high resistance to swelling. Little *et al.* found also that the matrix of the mechanically alloyed steel was stable to radiation–induced phase transformation; no changes were observed in the distribution of the chi–phase particles present before irradiation, although very fine scale effects could not be ruled out.

## NICKEL MODIFIED MA957

MA957 has a chemical composition which was originally formulated to ensure a ferritic microstructure for the sake of void swelling resistance during neutron irradiation. The Fe–Cr phase diagram shows a classical $\gamma$–loop *i.e.* the austenite phase field is enclosed in such a way that beyond a certain critical concentration, the ferrite remains the stable phase to the melting temperature. It has been discovered recently that the composition of conventional MA957 is

| Alloy | Cavity Concentration / $10^{21}$ m$^{-3}$ | Cavity Diameter / nm | Cavity Swelling % | Dislocation Density / $10^{14}$ m$^{-2}$ |
|---|---|---|---|---|
| DT2203Y05 | 8.0 | 8.3 | 0.24 | 9.7 |
| AISI 410 | 19.8 | 6.0 | 0.49 | 8.9 |

Table 9: Results of experiments in which the samples were irradiated with chromium ions and $\alpha$ particles to a total displacement dose of 50 dpa and a helium content of 600 appm [10]. The alloy DT2203Y05 was induction annealed at 1050 $^\circ C$ for 3 minutes, followed by ageing at 800 $^\circ C$ for 24 hours. It is not clear whether this heat treatment is sufficient to give a recrystallised microstructure.

such that it just clips the $\gamma$–loop at around 1000 °C, so that it is possible with suitable heat treatment to obtain a few percent of austenite [16].

Calculations have demonstrated that the addition of just $\frac{1}{2}$ wt.% of nickel to the conventional alloy can raise the maximum austenite volume fraction to 0.5. Thus, a transformable mechanically alloyed steel, "MA957Ni" should be possible without any major changes in alloy chemistry.

Such alloys have now been made [47] and have confirmed the phase stability calculations. In fact, a series of four experimental alloys are available with a maximum austenite fraction from 0-1. The transformations have been detected experimentally. The possibility of generating a variety of microstructures by transformation has also been demonstrated.

## COLD DEFORMATION

Regle and Alamo [48] have conducted extensive studies on the recrystallisation behaviour of MA956 and MA957, for samples which were cold deformed after extrusion. Two deformation processes were used, swaging and drawing, with reductions ranging from 10 → 60%.

Swaging and drawing led to quite different changes in crystallographic texture, and indeed to the subsequent recrystallisation behaviour. In all cases, deformation led to a reduction in the recrystallisation temperature, the change being largest for the cold–drawn samples. For MA957, the maximum reduction in the recrystallisation temperature was found to be about 200 °C from 1450 → 1250 °C. The corresponding maximum reduction for MA956 was for the cold drawn samples, where the recrystallisation temperature could be reduced from 1350 → 750 °C.

Chou [47] has measured the stored energies in the samples studied by Regle and Alamo. Surprisingly, he found no increase in stored energy with deformation; indeed, it appears that

| MA957 | Recrystallisation Start, °C | Recrystallisation Finish, °C | Stored Energy $J\,g^{-1}$ |
|---|---|---|---|
| 0% drawn | 1370 | 1412 | 0.93 |
| 30% drawn | 1018 | 1093 | 0.78 |
| 40% drawn | 998 | 1056 | 0.70 |
| 50% drawn | 989 | 1041 | 0.69 |
| 60% drawn | 980 | 1027 | 0.65 |

Table 10: Cold drawn MA957. DSC measurements at 20 K $min^{-1}$ (after Chou, unpublished research)

the deformation leads to a reduction in stored energy (Table 10).

There is no clear explanation of the results, but it is possible that the cold deformation modifies the crystallographic texture. It is conceivable that the texture change both leads to a reduction in the stored energy, and at the same time, a reduction in the recrystallisation temperature. The texture could, for example, lead to the clustering of adjacent grains into similar orientations. This would lead to an increase in the effective grain size, thereby making the nucleation of recrystallisation more easy.

There are some other elegant results presented by Regle and Alamo, which are consistent with this interpretation. A sample which was necked by deformation (and hence contained a controlled deformation gradient), was subjected to a recrystallisation heat treatment. It was vividly demonstrated that the anisotropic recrystallisation grain structure became refined with the extent of deformation. This is in spite of the fact that the stored energy actually decreased. Thus, deformation must enhance the nucleation rate of recrystallisation, perhaps by the texture mechanism discussed above.

## TRANSFORMATION PLASTICITY

Phase transformation under the influence of an external stress can cause plasticity. This non–recoverable strain is not to be confused with creep; transformation plasticity can occur at temperatures and in time–scales which are wholly inconsistent with the generation of detectable creep strains.

MA957 is, within a restricted temperature range, able to transform to a few percent of austenite. However, modifications of MA957 which are able to transform to a much greater extent, are found to be much more susceptible to transformation–induced plasticity [49]. Applications in which these modified alloys undergo cyclic transformation under the influence of stress are unlikely to be reliable.

## NONUNIFORM RECRYSTALLISATION

Most of the work in this area is on the nickel–base superalloy MA6000 [18]. It is found that there are profound differences across the cross section of the extruded bar, the edge regions recrystallising more easily relative to the core regions. The recrystallised grains tend to be have much larger aspect ratios at the edges. It appears that these differences are caused by inhomogeneous deformation. The oxide particles are more aligned along the extrusion direction at the regions near the surface, presumably because of the more extensive deformation in those regions. This alignment explains the greater anisotropy in the recrystallised grains and the relative ease of recrystallisation. The boundary mobility along the extrusion direction is larger when the particles are aligned. Stored energy measurements confirm that the observed effects cannot be explained by differences in the driving force for recrystallisation.

Martin [50] has discussed this work by presenting a calculation which indicates that the yttria particles, because of their small size, are not amenable to alignment by extrusion. However, Murakami *et al.* [51] have pointed out that his analysis assumes that the starting powder stock is uniform. This is not the case in practice. Mechanical alloying is a difficult process, and there are composition variations between powder particles/aggregates, which develop into banded regions as a consequence of extrusion. Results confirming the fact the mechanical alloying process can produce dispersoid inhomogeneities, which are carried through to the final product have recently been published by Jaeger and Jones [52,53] for alloys ODM 331 and ODM 751, both of which are iron based. This study is particularly useful in that the materials were examined both before and after consolidation. When a powder which is inhomogeneous in its dispersoid distribution is fabricated into a tube form, the particles align in concentric cylinders parallel to the tube axis. This in turn leads to an onion–peel type of recrystallised grain structure [53], which may be of some benefit from the point of view of mechanical properties.

It is strange that such inhomogeneities are most pronounced with the iron base alloys but not with the nickel base materials where the extent of particle alignment along the extrusion direction is usually minimal [16].

Finally, it is well established that both the manufacture of mechanically alloyed powder and the subsequent consolidation are both imperfect processes and lead to inhomogeneities in the final product. Fragments of improperly alloyed particles can be retained in the product, and act as defects [54]. If improperly bonded, they can act as cavities, or indeed as pinning centres for the advancing recrystallisation front.

## MA956 SHEET

MA956 sheet has the same composition as its rod form, but is made by a different route. After consolidating the mechanically alloyed powder by hot isostatic pressing, the billets are hot rolled with a reduction of approximately 98% to a thickness of 2.1 cm [55]. The rolling is carried out in the temperature range 1025–1065 °C.

The sheet is often cold deformed (typically another 60% reduction in thickness) before a recrystallisation heat treatment at about 1340 °C. The recrystallisation then begins at the centre of the sheet – in fact, the central regions tend to recrystallise completely before the surface regions [55]. The reason for such behaviour is not understood.

The crystallographic texture after the hot–deformation is {100} < 011 >, a texture which is sharpened by deformation at ambient temperatures [55].

## RECRYSTALLISATION FRONT DUE TO ZONE ANNEALING

Directional recrystallisation during zone annealing can occur at a front which separates the recrystallised and unrecrystallised portions of the bar. The nature of the front has been characterised in MA6000 [56], in MA957 [14,33,57] and in MA956 [14]. Of these alloys, MA956 is exceptional in that the recrystallisation front is irregular (Fig. 7), extending over large distances along the zone annealing direction. The other alloys have a smooth recrystallisation front, which tends to be curved, the front advancing at a higher rate at the sample surface compared with the centre of the bar.

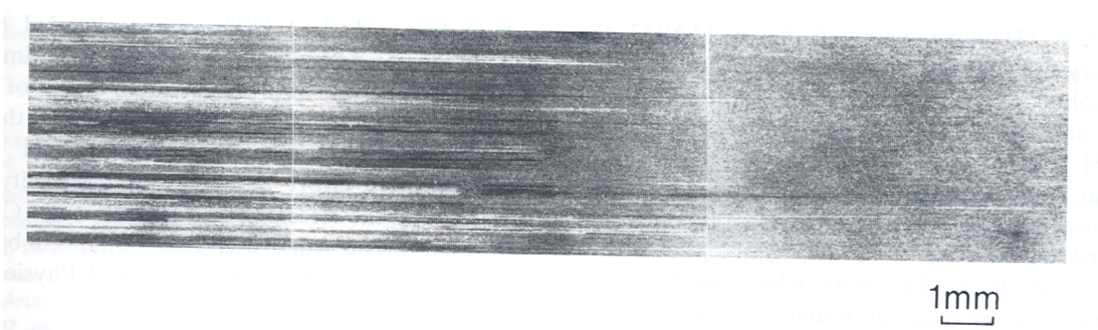


Fig. 7: An optical micrograph showing the spiked recrystallisatin front of a partially recrystallised sample of MA956

There are a number of explanations for this curvature in the recrystallisation front. Heat penetrates through the surface so that the recrystallisation process at the surface should be at a more advanced stage relative to the central regions. Miodownik *et al.* [57] carried out an experiment in which a partially zone annealed sample was subsequently held in a stationary temperature gradient for thirty minutes. Since the recrystallisation front remained curved, they claimed that the curvature cannot be explained by temperature gradients normal to the zone annealing axis. However, the degree of curvature in fact decreased on holding the sample in the stationary temperature gradient. The possibility therefore remains that temperature variations across the cross section of the bar are to some extent responsible for the curvature in the recrystallisation front.

In the specific case of a nickel–base superalloy MA6000, Murakami *et al.* [18] have shown that the extrusion process leads to a greater degree of dispersoid alignment in the surface regions of the bar, and that this leads to a greater ease of recrystallisation in those regions. This could also explain the curved recrystallisation front. By contrast, Marsh and Martin [56] ascribed the curved front to the existence of strain (and corresponding texture) gradients in the MA6000 bar. It is worth noting that although it is likely that the extrusion process leads to a greater degree of deformation in the surface regions, the stored energy of the MA6000 does not vary significantly across the cross–section [18] because the sample is in the primary recrystallised state before zone annealing.

Evens *et al.* [33] have suggested that in MA957, the curved recrystallisation front is a consequence of gradients in solute concentration, which influence grain boundary mobility. In support of this idea, Miodownik *et al.* [57] showed a peak in the concentration of titanium at a grain boundary in an extruded and heat treated bar of MA957. An experiment like this needs to be repeated on an unrecrystallised sample, since it is solute segregation in that state which needs to be characterised, rather than at boundaries between the coarse directionally recrystallised grain boundaries.

## COMPOSITE ALLOYS

Since MA956 is so heavily alloyed with aluminium and chromium, its ferritic matrix remains stable until the melting temperature. It is therefore not possible to control its grain structure using the $\gamma \rightarrow \delta$ transformation. A feasible alternative could be to introduce a fraction of transformable material within the powder compact of MA956 before it is extruded. This amounts to making the alloy chemically inhomogeneous, a metallic composite dubbed MeMeC (metal–metal–composite). The transformable part can in principle help control the grain structure of the residue which does not transform.

Work in this area is in its early stages, but initial results show that it is possible to obtain fine grained microstructures in MA956–20% MA957Ni composites.

## SUMMARY

Recrystallisation in MA–ODS iron and nickel–base alloys is dominated by the ultra–fine grain structure which is a consequence of the mechanical alloying and consolidation process, and by the presence of dispersoids. The grain structure can be so fine that the grain junctions themselves act to hinder the initiation of recrystallisation. Such fine grains cannot be considered to be topologically independent in this context. The dispersoids are mainly responsible for the anisotropy in the recrystallisation microstructure.

In general, the microstructure of these alloys is well–characterised and understood. It is necessary now to gain an equal understanding of the mechanical properties of such alloys.

**ACKNOWLEDGMENTS**

The author is grateful to Professor A. H. Windle for the provision of laboratory facilities at the University of Cambridge and to Dr. David Gooch for commenting on several drafts of the paper. I am also grateful to H. Harada, G. Hack, J. O'Driscoll, L. Patel, J. O'Driscoll, T. Chou, K. Murakami, K. Mino, A. Badmos and W. Sha for many helpful discussions. Some of this work was carried out under the auspices of the "Atomic Arrangements: Design and Control Project", which is a collaborative effort between the University of Cambridge and the Research and Development Corporation of Japan. The work was also supported by National Power plc. and the Engineering and Physical Sciences Research Council.

**REFERENCES**

1. J. S. Benjamin and P. S. Gilman: *Metals Handbook,* ninth edition, ASM International, Ohio **7** (1983) 722.
2. G. H. Gessinger: *Powder Metallurgy of Superalloys,* Butterworth and Co., London. (1984)
3. G. A. J. Hack: *Powder Metallurgy* **27** (1984) 73–79.
4. J. S. Benjamin: *Metall. Trans.* **1** (1970) 2943–2951.
5. H. Regle: *Ph.D. Thesis,* "Alliages Ferritiques 14/20% de chrome Renforces par Dispersion d'Oxydes", Universite de Paris–Sud. (1994)
6. P. Krautwasser, A. Czyrska–Filemonowic, M. Widera and F. Carsughi: *Materials Science and Engineering A* **A177** (1994) 199–208.
7. B. Kazimierzak, M. Prignon, C. Lecomte–Mertens and C. Coutsouradis: *High Temperature Materials for Power Engineering 1990,* Kluwer Academic Publishers, (1990) 131, quoted by Regle (1994).
8. L. Patel: *Private Communication,* to H. K. D. H. Bhadeshia, University of Cambridge, U. K. (1994)
9. W. Sha and H. K. D. H. Bhadeshia: *Metallurgical and Materials Transactions A* **25A** (1994) 705–714.
10. E. A. Little, D. J. Mazey and W. Hanks: *Scripta Metall. Mater.* **25** (1991) 1115–1118.
11. M. Takahashi and H. K. D. H. Bhadeshia: *Materials Science and Technology* **6** (1990) 592–603.
12. H. K. D. H. Bhadeshia: *Mathematical Modelling of Weld Phenomena III,* eds H. Cerjak and H. K. D. H. Bhadeshia, Institute of Materials, London (1996) in press.
13. D. Turnbull: *Metall. Trans. A* **12A** (1981) 695–708.
14. M. Baloch: *Ph.D. Thesis,* University of Cambridge. (1989)
15. M. Baloch and H. K. D. H. Bhadeshia: *Materials Science and Technology* **6** (1991) 1236–1246.
16. T. S. Chou and H. K. D. H. Bhadeshia: *Materials Science and Technology* **9** (1993) 890–897.
17. T. S. Chou and H. K. D. H. Bhadeshia: *Materials Science and Engineering A* **A189** (1994) 229–233.
18. K. Murakami, K. Mino, H. Harada and H. K. D. H. Bhadeshia: *Metall. Trans. A* **24A** (1993) 1049–1055.

19. Y. G. Nakagawa, H. Terashima and K. Mino: *Superalloys 1988,* eds S. Reichman, D. N. Duhl, G. Maurer, S. Antolovich and C. Lund, TMS–AIME, Warrendale, PA, U.S.A. (1988) 81–89.
20. K. Mino, Y. G. Nagakawa and A. Ohtomo: *Metall. Trans. A* **18A** (1987) 777.
21. K. Kusunoki, K. Sumino, Y. Kawasaki and M. Yamazaki: *Metall. Trans. A* **21A** (1990) 547.
22. K. Mino, H. Harada, H. K. D. H. Bhadeshia and M. Yamazaki: *Materials Science Forum* **88–90** (1992) 213–220.
23. P. Jongenburger: *Ph.D. Thesis no. 773,* Ecole Polytechnique Federale de Lausanne, Switzerland (1988)
24. A. P. Backhouse, S. S. Babu, K. Mino and H. K. D. H. Bhadeshia: *Pt. II Project Report,* Cambridge University. (1991)
25. K. Murakami: *Ph.D. Thesis,* Cambridge University. (1993)
26. J. H. Holloman and L. D. Jafee: *Trans. AIME* **162** (1945) 223–249.
27. P. J. Alberry and W. K. C. Jones: *Metals Technology* **4** (1977) 557–566.
28. M. F. Ashby and K. E. Easterling: *Acta Metall.* **30** (1982) 1969–1978.
29. W. Sha and H. K. D. H. Bhadeshia: *Materials Science and Engineering A* (1996) these proceedings.
30. K. Murakami and H. K. D. H. Bhadeshia: *Unpublished research,* Cambridge University. (1993)
31. A. Alamo, H. Regle and J. L. Bechade: *Novel Powder Processing,* Advances in Powder Metallurgy and Particulate Materials – 1992, Metal Powder Industries Federation, Princeton, NJ, USA **7** (1992) 169–182.
32. T. S. Chou and H. K. D. H. Bhadeshia: *Metall. Trans. A* **24A** (1993) 773–779.
33. P. J. Evens, J. W. Martin and E. A. Little: *Materials Science and Technology* **8** (1992) 531–536.
34. G. B. Schaffer, M. H. Loretto, R. E. Smallman and J. W. Brooks: *Acta Metall.* **37** (1989) 2551–2558.
35. H. Cama and T. A. Hughes: *Institute of Physics Conference Series No. 138: Section 7,* EMAG93, ed. A. Craven, IOP Publishing, Oxford, U. K. (1993) 361–364.
36. V. C. Nardone and J. K. Tien: *Scripta Metallurgica* **17** (1983) 467.
37. R. S. Herrick, J. R. Weertman, R. Petkovic–Luton, and M. J. Luton: *Scripta Metallurgica* **22** (1988) 1879.
38. J. H. Schroder and E. Arzt: *Scripta Metallurgica* **19** (1985) 1179.
39. J. Preston, B. Wilshire and E. A. Little: *Scripta Metall. Mater.* **25** (1991) 183–184.
40. R. W. Evans, J. Preston, B. Wilshire and E. A. Little: *J. of Nuclear Materials* **195** (1992) 24–28.
41. H. Nickel and W. J. Quadakkers: *Heat Resistant Materials* eds. K. Natesan and D. J. Tillack, Fontana, WI, Sept. 1991, ASM International (1991) 87.
42. I.–G. Lee, A. K. Ghosh, R. Ray and S. Jha: *Metallurgical and Materials Transactions* **25A** (1994) 2017–2026.
43. D. L. Whittenberger: *Metallurgical Transactions A* **12A** (1981) 845.
44. D. M. Jaeger and A. R. Jones: *Materials for Combined Cycle Power Plant,* Institute of Metals, London (1991) 1–11.
45. K. Murakami, H. Harada and H. K. D. H. Bhadeshia: *Heat Treatment '92,* ed. I. Tamura, Kyoto, Japan (1992) 269–272.
46. E. A. Little: *Materials Modelling: From Theory to Technology,* IOP Publishing, Oxford (1991) 141–146.

47. T. S. Chou: *Ph.D. Thesis,* University of Cambridge. (1994)
48. H. Regle and A. Alamo: *Journal de Physiqe IV* **3, C7** (1993) 727–730
49. S. Suzuki and H. K. D. H. Bhadeshia: *Unpublished research,* Cambridge University. (1993)
50. J. W. Martin: *Metallurgical Transactions A* **25A** (1994) 651–652.
51. K. Murakami, K. Mino, H. Harada and H. K. D. H. Bhadeshia: *Metall. Trans. A* **25A** (1994) 652–653.
52. D. M. Jaeger and A. R. Jones: *Materials for Advanced Power Engineering,* "Dispersoid distributions in iron based ODS alloys made by mechanical alloying", Leige, Belgium (1994) in press.
53. D. M. Jaeger and A. R. Jones: *Materials for Advanced Power Engineering,* "The development of grain shape in iron base ODS alloys", Leige, Belgium (1994) in press.
54. D. M. Jaeger and A. R. Jones: *Processing, Properties and Applications of Metallic and Ceramic Materials,* eds. M. H. Loretto and G. J. Beevers, Birmingham, U. K. (1992) 1–6.
55. R. C. Klug, G. Krauss and D. K. Matlock: *Hot Deformation Textures and Microstructures,* TMS Fall Meeting, November 1993, Pittsburgh, PA, unpublished research. (1993)
56. J. M. Marsh and J. W. Martin: *Materials Science and Technology* **7** (1991) 183.
57. M. A. Miodownik, J. W. Martin and E. A. Little: *Journal of Materials Science Letters* **12** (1993) 834–835.

. Y. Ikeda, H. Sumiyoshi and Y. Ishiwata: *ISIJ International* **35** (1995) 1109–1114.

. Y. Kawasaki, Y. Ikeda, T. Kobayashi and H. Sumiyoshi: *ISIJ International* **36** (1996) 1208–1214.

. M. F. Hupalo, M. Terada, A. M. Kliauga and A. F. Padilha: *Mat.–wiss. u. Werkstofftech.* **34** (2003) 505–508.